

**A VORTEX CONTROL TECHNIQUE FOR THE ATTENUATION  
OF FIN BUFFET**

David E. Bean, Douglas I. Greenwell and Norman J. Wood

School of Mechanical Engineering  
University of Bath  
Bath, England

**ABSTRACT**

The application of Tangential Leading Edge Blowing to reduce levels of single fin buffeting has been studied. The tests were performed at the University of Bath 2.1m x 1.5m Wind Tunnel using two cropped 60° delta wings. To measure the buffet excitation, a rigid fin instrumented with miniature differential pressure transducers was used. A flexible fin of similar planform and size was used to measure the buffeting response. Steady state static pressure data and laser light sheet flow visualisation were employed to aid interpretation of the vortical flow over the wings, and hence identify the causes of the buffeting. The profiles of the buffet excitation and response were found to match each other very closely.

It was observed that symmetric leading edge blowing modified the leading edge vortices by reducing the 'effective angle of attack' of the vortex. Blowing at a constant rate shifted the buffet excitation and response to higher angles of attack. Flow visualisation confirmed that the mechanism at peak buffeting had not changed, but had been merely shifted. It has been shown that the use of an optimum blowing profile could completely suppress the buffeting response without impairing the wing lift characteristics.

**NOMENCLATURE**

$\bar{c}$	Wing Mean Aerodynamic Chord, (0.36m)
$C_\mu$	Blowing Momentum Coefficient (Jet Momentum / qS)
f	Frequency
K	Reduced Frequency ( $f\bar{c}/U$ )
m	Generalised Mass
$\sqrt{nG(n)}$	Buffet Excitation Parameter
$\bar{p}$	rms Pressure Fluctuation
q	Free Stream Dynamic Pressure
S	Wing Reference Area
$S_f$	Fin Reference Area
U	Tunnel Free Stream Velocity
z	Fin Tip Acceleration (rms)
$\alpha$	Angle of Attack
$\beta$	Sideslip Angle
$\zeta$	Total Damping (fraction of critical)
$\theta$	Pitch Angle
$\phi$	Roll Angle

**Abbreviations**

LDV	Laser Doppler Velocimetry
LEX	Leading Edge eXtension
TLEB	Tangential Leading Edge Blowing

**INTRODUCTION**

High angle of attack and post-stall manoeuvring continues to be a factor in the design of future generation combat aircraft<sup>[1][2]</sup>. It is anticipated that future combat aircraft will be required to maintain controlled flight in the high angle of attack regime for extended periods.

Severe fin buffeting has been encountered on this type of aircraft (both single and twin finned) during operation at high angles of attack. From wind tunnel and flight tests performed on such aircraft<sup>[3][4]</sup>, the buffeting has been attributed to vortex flow enveloping the fin(s), which excites the natural frequencies of the fin structure. This phenomenon not only decreases the fatigue life of the airframe, but may also limit the angle of attack envelope of the aircraft. Clearly this is an undesirable situation which must be considered early in the design of advanced combat aircraft.

At present the most common fin buffet attenuation technique is structural reinforcement. This reduces the vibration of the fin at the expense of increased overall weight, and hence decreased aircraft performance. This method is only remedial, since it does not seek a solution to the cause of the buffeting.

Several studies have been performed to reduce the buffeting by affecting the excitation at source, i.e. where the vortices are generated. The concept of applying suction at the forebody apex to control the forebody vortices at high angles of attack<sup>[5]</sup> was examined on a representative aircraft model with a single fin configuration. It was found that nose suction altered the position of the forebody vortices away from the fin, and thus decreased the levels of fin buffeting. Hence it is possible to reduce buffeting by manipulation of the vortices that excite the structure.

The use of a LEX fence to reduce fin buffeting on the F/A-18 has been well documented<sup>[6][7]</sup>. Buffeting levels were decreased by around 10%-15% (rms) and minimal performance penalties were incurred, thus confirming the LEX fence as a practical means of buffet prevention for LEX vortex induced buffeting. However, this method of buffet suppression is highly geometry dependent, since the effectiveness of the fence is expected to be sensitive to small changes in fence position.

Another study of F/A-18 fin buffeting<sup>[8]</sup> showed that the excitation flowfield was concentrated at a distinct frequency, which varied linearly with free stream velocity. It was noted that there was a good correlation between the normalised excitation pressures and fin accelerations, and that the maximum fin response (at a given angle of attack) occurred when the dominant frequency of the pressure field and the fin natural frequency were approximately matched.

The purpose of this paper is to introduce a different method of buffet suppression using the concept of Tangential Leading Edge Blowing (TLEB). Preliminary investigations have been performed to assess the merit of TLEB for buffet alleviation for a single finned aircraft configuration<sup>[9]</sup>. Although the wing leading edge (and hence the jet profile) was not ideal, and values of the blowing momentum coefficient ( $C_{\mu}$ ) were not obtained accurately, the system provided some buffeting reduction. It was also noted that the system gave a slight improvement in the drag at high angles of attack. Therefore TLEB has potential for suppressing buffeting at high angles of attack whilst providing improvements in aircraft performance.

Recent studies at the University of Bath have demonstrated the ability of TLEB to control the vortical flowfield on delta wings in the post-stall region<sup>[10]</sup>. The present study includes measurements of buffet levels on a flexible fin and unsteady pressures on a rigid fin of similar planform, for both unblown and blown 60° delta wings. Laser light sheet flow visualisation and force/moment balance tests have been conducted to clarify the mechanisms for buffeting reductions using TLEB.

### TANGENTIAL LEADING EDGE BLOWING

Previous research has demonstrated the ability of TLEB to modify vortical flowfields and to provide lateral control at both pre-stall and post-stall angles of attack<sup>[11][12]</sup>. TLEB is an application of the phenomenon of Coanda jet attachment to convex surfaces.

If the leading edge of a delta wing is sharp, the leading edge separation point is fixed, and the vortex equilibrium condition is influenced only by the vortex strength and position for a given angle of attack. However if the leading edge is rounded, the separation point is able to move around the leading edge, providing an additional degree of freedom on the flowfield. Therefore there exists a unique vortex strength and location for each leading edge separation point at a constant angle of attack. By injecting a thin tangential jet into the crossflow boundary layer near the leading edge (see figure 1), further control of the boundary layer separation is provided by the momentum of the jet, so the jet enables control of the vortex equilibrium condition at a given angle of attack.

At low angles of attack, the effect of TLEB is to reduce the leading edge vortex strength and re-locate the vortex inboard with negligible reduction in wing normal force. At post-stall angles of attack, blowing moves the vortex burst points aft, and augments the wing normal force. TLEB can be considered as reducing the "effective angle of attack" of the vortex, i.e. at fixed incidence, increasing blowing momentum modifies the vortical flow to represent that present at a lower angle of attack.

## EXPERIMENTAL APPARATUS

### Model Support System

A model support system has been designed to be used in the 2.1m x 1.5m tunnel at the University of Bath, specifically for research into high angle of attack aerodynamics (figures 2 and 3). The rig is a pantograph mechanism mounted on its side with pitch control provided by an electric linear actuator which provides a pitch range from 0° to 90°. With an integral roll shaft (capable of ±180°), the system offers a ±90° capability in both model angle of attack and sideslip using the following relationships<sup>[10]</sup>:

$$\alpha = \tan^{-1}(\cos\phi.\tan\theta)$$

$$\beta = \sin^{-1}(\sin\phi.\sin\theta)$$

The model is sting mounted on an "A-frame" layout to give maximum lateral stiffness, and model forces and moments are measured by a 3-component strain gauge sting balance.

The horizontal pantograph mechanism has several advantages over more conventional sting mounted systems:

- (i) The model pitches about its centre of area on the tunnel centreline, thus reducing asymmetric blockage and simplifying LDV measurements and laser light sheet flow visualisation. The maximum solid blockage for the current models under test is 5% at 90° angle of attack.
- (ii) Rig actuation loads are small, since it is not necessary to support the weight of the model when pitching up or down.
- (iii) At high angles of attack, the sting assembly is clear of the model wake, reducing any downstream interference. Model supports have been shown to have a significant effect on vortical flows in wind tunnels<sup>[13]</sup>.
- (iv) Under aerodynamic load, the "A-frame" arms deflect similarly, giving negligible change in pitch angle.
- (v) As the model pitches horizontally across the "long" axis of the tunnel, the sting balance zeroes remain constant, simplifying the wind-off calibration procedure.

Glass panels in the tunnel walls provide laser access, and all Scanivalve tubing, instrumentation wires and blowing air supplies are passed inside the "A-frames".

### Wind Tunnel Models

Two models of similar planform and size, one with and one without TLEB, have been built and tested to determine the effects of TLEB on buffeting response. Both models are 60° delta wings of 0.5m span, with a trailing edge extension for fin attachment. The unblown wing has a rounded leading edge, 4% thickness, and is fitted with 90 upper surface pressure tappings situated at x/c= 0.30, 0.45, 0.59, and 0.73 .

The blown wing is 3% thick and has two separate plenum chambers providing the blowing supply for the slots, which extend over the majority of the leading edges. The plenum pressures are monitored separately by miniature pressure transducers, and manually controlled. The leading edge slot height is adjustable from 0.0mm - 1.0mm, and may vary along the slot length. Previous experience has shown that TLEB is most efficient when a linear tapered slot is used<sup>[14]</sup> (tapering towards the wing apex). This slot configuration gives results that are easiest to interpret, as the vortical flow responds quasi-conically. Two slot configurations were tested ; a linear tapering slot and a constant width slot.

The buffeting response was measured using a flexible fin, whose natural frequencies were designed using the following reduced frequencies (based on wing mean aerodynamic chord and half the maximum tunnel velocity):

Bending (1st Mode) ,  $K = 0.6$  to  $0.8$ ;  
Torsion (1st Mode) ,  $K = 2.0$  to  $3.0$ .

These reduced frequencies are typical of a modern combat aircraft. The frequency term in this expression is the frequency of the natural mode (and therefore unrelated to the excitation frequency). The flexible fin is shown in figure 4. It consists of a thin brass spar, surrounded by a balsa wood shroud to provide an aerodynamic fairing and the correct fin area. Fin vibration levels were sensed by root strain gauges, instrumented in half-bridge circuits.

The fin used to detect the excitation pressures was rigid, manufactured from aluminium, and of similar planform and section to the flexible fin. A miniature differential pressure transducer was mounted on each face of the fin at 75% span and 40% chord, to monitor the pressure fluctuations in the flow.

Both fins were rigidly fixed to the trailing edge extensions of the models. Typical test Reynolds Numbers were  $0.8 \times 10^6$  based on wing root chord.

Laser light sheet flow visualisation was used to help understand the phenomenon of buffeting. Laser access was via the wind tunnel door and floor windows, with smoke injected on the lower surfaces of the wings adjacent to the leading edge. Images were obtained using both a 35mm camera and a low light level video camera.

#### Data Acquisition and Reduction

On-line data acquisition and reduction of the strain gauge balance data and steady state pressures was performed using a data acquisition program "Rigtest3.3" developed at the University of Bath. The program was written specifically to control the DT2821<sup>®</sup> data acquisition board (by Data Translation Inc.), which was installed on a desktop computer.

The steady state pressures were measured by two standard J-type Scanivalves. The tunnel reference pressure was acquired from a digital micromanometer and the model attitude could be set under program control. All data was displayed graphically in coefficient form immediately after being acquired.

The unsteady fin buffeting data (from the strain gauges and pressure transducers) was gathered using a commercially available data acquisition package (Global Lab<sup>®</sup> by Data Translation Inc.) which controlled a DT2821<sup>®</sup> data acquisition board. After acquisition, the data could be manipulated (using Global Lab's extensive analysis library) and saved as post processed results. Available signal conditioning functions include fourier transforms, power spectra, correlation and filtering techniques.

The fin excitation and response data were non-dimensionalised in order to enable comparison between different test configurations. The response (strain gauge) data was reduced into the non-dimensional buffet parameter<sup>[15]</sup>:

$$\sqrt{nG(n)} = \frac{2 m z}{\sqrt{\pi} q S_f} \sqrt{\xi}$$

where  $m$  is the generalised mass,  $z$  is the rms tip acceleration and  $\xi$  the total damping (measured as the fraction of critical).

The generalised mass was determine using modal analysis. A known impulse was applied to the fin structure using an instrumented hammer, and a light accelerometer sensed the natural modes present. The mass term for each natural mode was then derived from the spectra of both signals.

Buffeting spectra were obtained from within Global Lab using an FFT size corresponding to 6-7 seconds of raw data. The total damping values (typically 2%-3%) were derived using the half power method, and were found to be independent of free stream speed, indicating that the damping was predominantly structural.

The excitation (unsteady pressure) data was non-dimensionalised into the form

$$\bar{p}/q$$

where  $\bar{p}$  is the total broad-band rms pressure fluctuation. This parameter represents the oscillatory nature of the flow at the fin surface.

### RESULTS AND DISCUSSION

All results presented correspond to buffeting tests at zero wing sideslip and a reduced frequency of 0.6 (based on the fin 1st bending and wing mean aerodynamic chord), except where stated.

#### Unblown Baseline Results

The single fin response in the fundamental bending mode (32Hz) is shown in figure 5. For low angles of attack the response is small, the vortices lie away from the fin, and the fin excitation is a result of general flow unsteadiness. At  $\alpha=34^\circ$  (a point called 'buffet onset') the buffeting increases from this baseline value, up to a sharp peak at  $\alpha=43^\circ$ . The response then falls with increasing angle of attack to reach a fairly constant level, the fin being in the wake of the fully stalled wing (like that of a bluff body). When compared to normal force data for the same wing, it is evident that the point of maximum buffeting occurs in the

post-stall region. No significant buffeting was recorded in either the 1st torsional mode or the 2nd bending mode at this tunnel speed.

The excitation, represented by the rms pressure levels, corresponding to the above response is shown in figure 6. For  $\alpha < 34^\circ$  both port and starboard faces of the fin experience low levels of buffet excitation. The port face excitation then rises the quicker (perhaps due to some slight sideslip on the fin, or some tunnel swirl) to peak at  $\alpha = 43^\circ$ , whereas the starboard face excitation peaks at  $\alpha = 44^\circ$ . When compared with the buffeting response, it can be seen that the profiles of both sets of curves are very similar.

Typical unsteady pressure fluctuations for both faces of the rigid fin at  $\alpha = 44^\circ$  are shown in figure 7. It can be seen that the traces move in and out of phase regularly. When out of phase, one face of the fin experiences an instantaneous suction, and the other face experiences an instantaneous pressure (and vice versa). For a flexible fin, this would induce a side force and possibly a fin deflection.

This suggests that there is a direct energy transfer from the flow (in the form of pressure fluctuations) into the structure (in the form of fin deflection). A possible mechanism for this energy transfer can be deduced from the spectra of the excitation pressures. Figure 8a shows the power spectral density function corresponding to the point  $\alpha = 10^\circ$  in figure 6 (for the starboard face). It can be seen that the spectrum has no distinct resonant frequencies, and the overall excitation level is much less than figure 8b, which corresponds to the point  $\alpha = 44^\circ$ . The spectrum at peak buffeting reveals a broad-band excitation which decreases in intensity to the background level at around  $f = 200\text{Hz}$ . The absence of any torsional buffeting is due to the torsional natural frequency (192Hz) not lying within this excitation range. Conversely the bending response was large, since the natural mode was situated inside the excitation band. Thus a buffeting response in a natural mode will occur when the frequency of that natural mode lies within the excitation band of the corresponding flowfield.

The nature of the fin excitation pressures can be analysed by subtracting the pressure time trace corresponding to one face of the fin from the other. This subtraction emphasises the out-of-phase components of the pressure traces (and hence the differential pressure across the fin), and suppresses the effect of any in-phase components (Figure 7c).

Figure 9 shows a power spectral density curve of the buffet excitation trace (port pressure minus starboard pressure) corresponding to the point  $\alpha = 44^\circ$ . It can be seen that a peak occurs at approximately 35Hz. Hence for this model configuration, the spectra of individual pressure transducer outputs on each face of the fin show little distinct periodicity, yet the spectrum of the differential pressure does. Furthermore, the variation of peak vortex excitation frequency is linear with free stream velocity<sup>[8]</sup> (as expected).

Figure 10 presents the variation of excitation frequency with free stream velocity for several angles of attack. The curves are linear for all cases. Using a reduced frequency parameter incorporating the vortex excitation frequency ( $f_{\text{VORTEX}}$ ) and a nominal wake width ( $\bar{c} \sin \alpha$ ) it can be seen that the peak vortex excitation frequency can be expressed in the form

$\alpha$	$(f_{\text{VORTEX}} \bar{c} / U)$	$(f_{\text{VORTEX}} \bar{c} / U) \sin \alpha$
$35^\circ$	0.96	0.55
$38^\circ$	0.89	0.55
$41^\circ$	0.75	0.49
$44^\circ$	0.76	0.53

TABLE 1

$$\left[ \frac{f_{\text{VORTEX}} \bar{c}}{U} \right] \sin \alpha = \text{constant (for a given configuration)}$$

This parameter represents the frequency content of the vortical flow for this wing. Therefore this model configuration has a characteristic value of 0.55, in accordance with a recent study using wings of similar planform<sup>[16]</sup>. Frequency parameter tests using the flexible fin<sup>[17]</sup> also give a value of approximately 0.55 (Figure 11). This shows the variation of buffeting in the fundamental bending mode with free stream velocity. It can be seen that there is a peak in the response at approximately  $16\text{ms}^{-1}$ . When transferred onto Figure 10, it is evident that the dominant vortical flow frequency at  $\alpha = 44^\circ$  is almost identical to the frequency of the natural mode excited. This confirms that the maximum buffeting response (for a given angle of attack) occurs when the frequency of the excitation flowfield matches the structural mode frequency.

However, comparisons between different buffeting studies suggest that  $\bar{c} \sin \alpha$  is not an appropriate scaling parameter, since different values of the reduced frequency parameter are found (0.22<sup>[3]</sup>, 0.29<sup>[8]</sup><sup>[18]</sup> using unsteady pressures, and 0.71<sup>[19]</sup> using the response).

Laser light sheet flow visualisation was performed to establish the flow conditions at various buffeting levels. Figure 12a shows the starboard vortex located away from the fin at  $\alpha = 36^\circ$  (before peak buffeting). The port vortex is in the shade of the fin, and is therefore not illuminated. At  $\alpha = 43^\circ$  (figure 12b) it can be seen that the leading edge vortex core diameter has grown, and the vortex free shear layer is located on or near the fin tip<sup>[20]</sup>. Since the laser light sheet image represents a two-dimensional slice through the flow, it is necessary to consider the flow conditions three-dimensionally. As well as impinging on the fin tip, each vortex free shear layer impinges on the swept leading edge of the fin. Video recordings suggest that a vortex/fin interaction is present at maximum buffeting. When the port vortex contracts slightly, the starboard vortex expands (and vice versa) to maintain vortex equilibrium. This may relate to the  $180^\circ$  phase lag in the pressure fluctuations discussed earlier. Consequently, the shear layers oscillate across the fin leading edge and tip, resulting in large fin excitations.

Normal force data was acquired for the unblown wing, with and without the fin fitted. It was found that the fin had little effect on the force curves, with lift curve slopes and stall angles remaining constant. Also steady state static pressure data was taken at angles of attack before and after buffet onset. For all cases the flow was symmetrical (i.e. no vortex asymmetry), even at maximum buffeting<sup>[20]</sup>. These observations suggest that the presence of the fin has very little effect on the vortical flow over a delta wing at incidence, as the fin is situated away from either vortex.

## Effect of TLEB

### Parallel Slot Distribution

The parallel leading edge slot configuration had a constant slot height of 0.5mm. Figure 13 shows the single fin response in the fundamental bending mode for four different blowing momentum coefficients, ( $C_{\mu}$ ). For low angles of attack the effect of blowing is small, since the vortices are located away from the fin. At around  $\alpha=35^\circ$ , buffet onset occurs for all cases. The effect of TLEB is to reduce the rate of buffet increase after buffet onset, resulting in the buffeting peak being shifted to a higher angle of attack. As the amount of blowing applied increases the peaks are offset further from the baseline case with little change in the peak buffeting level. This supports the hypothesis that TLEB reduces the 'effective angle of attack' of the vortices. A shift of around  $8^\circ$  in the angle of peak buffeting was experienced using a  $C_{\mu}$  of 0.10.

The effect of  $C_{\mu}$  on wing normal force is presented in figure 14. It can be seen that the blowing also increases the potential angle of attack range of the wing by approximately  $8^\circ$  for  $C_{\mu}=0.10$ .

Laser light sheet flow visualisation (figures 15a and 15b) was performed to establish the flow conditions for each peak buffeting case. Figure 15a shows both leading edge vortex shear layers located on or near the fin tip for  $C_{\mu}=0.00$  (as discussed earlier). As the angle of attack and blowing increase ( $\alpha=47^\circ$ ,  $C_{\mu}=0.05$ ) the flow conditions remain similar (figure 15b), emphasising that the buffeting mechanism has been shifted to a higher angle of attack.

### Tapering Slot Distribution

The slot height for the tapered configuration varied linearly from 0.05mm near the wing apex to 0.45mm near the wing trailing edge. The response profiles for this slot distribution are shown in figure 16. In comparison with figure 13, it can be seen that both sets of curves exhibit the same trends. However, the angle of attack shift for a particular  $C_{\mu}$  is much greater when using the tapering slots as the conicality of the flow has been maintained. For example, for  $C_{\mu}=0.10$  the angle of attack shift is around  $8^\circ$  for the parallel slot distribution and around  $14^\circ$  for the tapering slot. The parallel slot distribution is less efficient as the slot height (and hence the jet momentum) is too large in comparison to the local wing span at the wing apex, and too small towards the wing trailing edge. Hence the linear tapering slot distribution is more efficient at modifying the leading edge vortex characteristics.

The solid line in Figure 16 represents the buffeting level corresponding to an optimum blowing profile. At  $\alpha=38^\circ$  the blowing is steadily increased to peak at  $\alpha=41^\circ$  (peak buffeting), resulting in lower buffeting levels. As the angle of attack increases further, the blowing is reduced gradually, until at approximately  $\alpha=48^\circ$  the blowing momentum coefficient is zero, and the buffeting returns to the unblown level. It is clear that the buffeting peak can be completely suppressed using such a blowing profile.

The effect of TLEB on the spectrum of the excitation pressure on the fin at  $\alpha=44^\circ$  is presented in figure 17. In comparison with the unblown spectrum, the blown spectrum still comprises large pressure fluctuations at frequencies less than 200Hz, but at reduced levels. Consequently, there is a reduction in the buffeting response. When the buffet excitation and response are compared it is evident that both have been shifted to higher angles of attack, confirming that TLEB has modified only the vortex characteristics.

Figure 18 shows the effect of symmetric TLEB on the vortex excitation frequency for a constant angle of attack of  $38^\circ$ . It can be seen that all curves are linear, and that the gradients of the lines increase with increasing  $C_{\mu}$ . The results corresponding to tests conducted at several angles of attack are presented below:

$\alpha$	$(f_{\text{VORTEX}} \bar{c}/U)$	$(f_{\text{VORTEX}} \bar{c}/U) \sin \alpha$
$38^\circ$	1.03	0.63
$42^\circ$	0.95	0.63
$46^\circ$	0.85	0.61
$50^\circ$	0.72	0.55

$\alpha$	$(f_{\text{VORTEX}} \bar{c}/U)$	$(f_{\text{VORTEX}} \bar{c}/U) \sin \alpha$
$38^\circ$	1.09	0.67
$42^\circ$	0.98	0.66
$46^\circ$	0.96	0.69
$50^\circ$	0.90	0.69

TABLE 2

Hence symmetric TLEB has shifted the vortex reduced frequency parameter to larger values to 0.62 ( $C_{\mu}=0.05$ ) and 0.68 ( $C_{\mu}=0.10$ ). Scaled upon the sine of the angle of attack, these new characteristic values correspond to reductions in the "effective angle of attack" of  $7^\circ$  and  $14^\circ$  respectively. These reductions compare favourably with the positive angle of attack shifts in the buffeting response, which were induced by the blowing. The shift of reduced frequency parameter is therefore equivalent to a reduction of the vortical flow angle of attack for a wing of given sweep.

An estimation of the quantity of air needed to provide TLEB for a full scale combat aircraft was performed. Scaled on the wing area, a blowing momentum coefficient of 0.10 would require less than 6% of the engine mass flow, based on a cruise at Mach 0.4 and the PW1120 engine. In practice this scaling law would result in an excessive slot height relative to the leading edge radius of the full size wing. The efficiency of the slot would be greatest if the ratio of slot height to leading edge radius was kept constant from model to full scale. Therefore the estimate of the amount of air needed is approximately four times too large.

## CONCLUSIONS

A system to suppress single fin buffeting on a simple delta wing has been designed, built and tested. Total suppression of fin buffeting may be achieved with a blowing rate equivalent to 1-2% of the total engine mass flow.

It has been shown that the frequency content of the excitation flowfield is a function of free stream velocity and angle of attack. The characteristic value of this function (for unblown single finned configurations) is approximately 0.55.

Symmetric TLEB induces a linear shift in the buffeting response and the wing stall angle. It was found that a tapering slot was almost twice as efficient at modifying vortex behaviour and hence suppressing fin buffeting, compared to a parallel slot.

The maximum response was characterised by both leading edge vortex shear layers impinging on the fin leading edge and tip.

## ACKNOWLEDGMENTS

This work was carried out with the support of DRA Bedford under contract 2112/80. Their support is greatly appreciated.

## REFERENCES

1. Herbst, W.B., "Future Fighter Technologies", Journal of Aircraft, Vol 17 No 8 pp 561-566, August 1980.
2. Orlik-Rückemann, K.J., "Aerodynamic Aspects of Aircraft Dynamics at High Angles of Attack", Journal of Aircraft, Vol 20 No 9 pp 737-752, September 1983.
3. Triplett, W.E., "Pressure Measurements on Twin Vertical Tails in Buffeting Flow", AIAA 82-0641.
4. Wentz, W.H. Jnr, "Vortex-Fin Interaction on a Fighter Aircraft", AIAA 87-2474.
5. Ross, A.J., Jefferies, E.B. and Edwards, G.F., "Aerodynamic Data for the Effects of Nose Suction on a High Incidence Research Model with a Large Forebody", RAE Technical Memorandum 2204, January 1991.
6. Lee, B.H.K. and Brown, D., "Wind Tunnel Studies of F/A-18 Tail Buffet", AIAA 90-1432.
7. Lee, B.H.K. and Brown, D., "Wind Tunnel Investigation and Flight Tests of Tail Buffet on the CF-18 Aircraft", AGARD CP-483, April 1990.
8. Martin, C.A. et al "F/A-18 1/9<sup>th</sup> Scale Model Tail Buffet Measurements", ARL Flight Mechanics Report 188, June 1991.
9. Mabey, D.G. and Pyne, C.R., "Reduction of Fin Buffeting by Tangential Blowing on the Leading Edge of a Wing", DRA Technical Memorandum 2215, May 1991.
10. Greenwell, D.I. and Wood, N.J., "Control of Asymmetric Vortical Flows", AIAA 91-3272.
11. Wood, N.J. and Roberts, L., "The Control of Delta Wing Aerodynamics at High Angles of Attack", Paper presented at "The Prediction and Exploitation of Separated Flows", Royal Aeronautical Society, April 1989.
12. Wood, N.J., "Development of Lateral Control on Aircraft Operating at High Angles of Attack", ICAS-90-5.6.3, 1990.
13. Johnson, J.L. Jnr, Grafton, S.B. and Yip, L.P., "Exploratory Investigation of the Effects of Vortex Bursting on the High Angle of Attack Lateral-Directional Stability Characteristics of Highly Swept Wings", AIAA 80-0463.
14. Wood, N.J., Roberts, L. and Lee, K.T., "The Control of Vortical Flow on a Delta Wing at High Angles of Attack", AIAA 87-2278.
15. Mabey, D.G., "Some Aspects of Aircraft Dynamic Loads due to Flow Separation", AGARD R-750, May 1988.
16. Chapman, M. and Cheeseman, J., "Vortex Burst Frequencies", School of Mechanical Engineering Report (University of Bath) AE10/92, April 1992.
17. Wood, N.J., "Suppression of Vortex Induced Unsteady Loads at High Angles of Attack", School of Mechanical Engineering Progress Report (University of Bath), October 1991.
18. Zimmerman, N.H. et al, "Prediction of Tail Buffet Loads for Design Application", AIAA 89-1378.
19. Mabey, D.G. and Pyne, C.R., "Buffeting on the Single Fin of a Combat Aircraft Configuration at High Angles of Incidence", RAE Technical Report 91006, January 1991.
20. Bean, D.E. and Wood, N.J., "An Experimental Investigation of Empennage Buffeting", AIAA 91-3224.

## Tangential Leading Edge Blowing

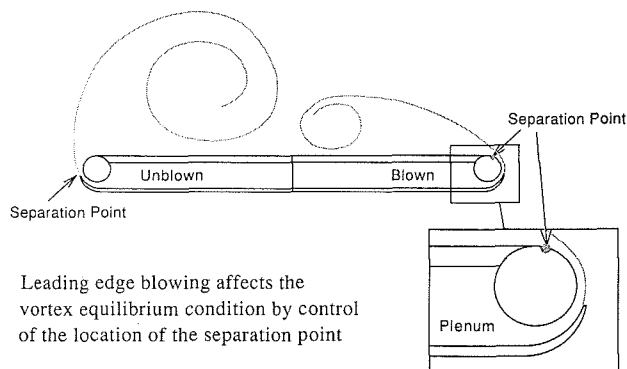


Figure 1: Tangential Leading Edge Blowing.

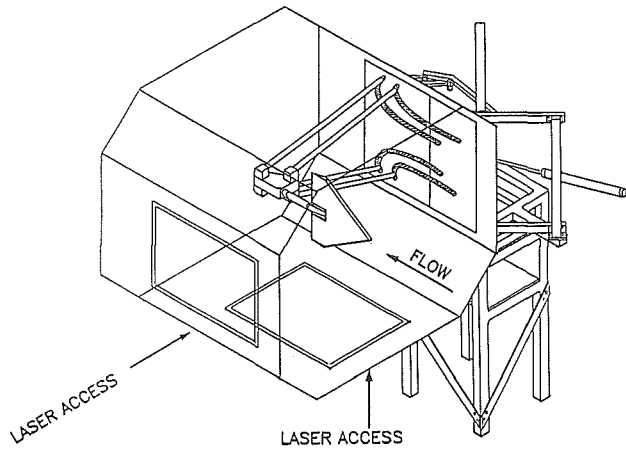


Figure 2: High Angle of Attack Model Support System in the 2.1m x 1.5m Low Speed Wind Tunnel.

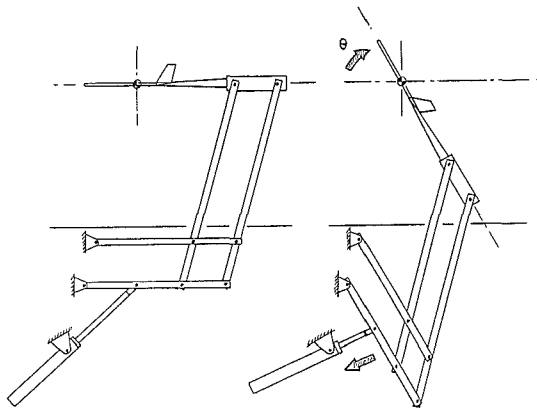


Figure 3: High Angle of Attack Model Support System Pitch Mechanism.

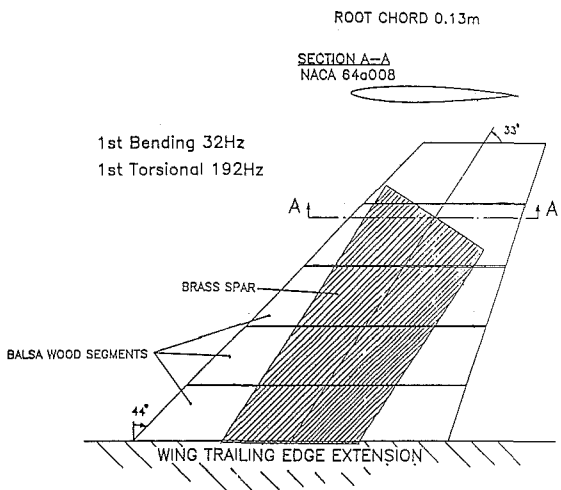


Figure 4: Flexible Fin Design.

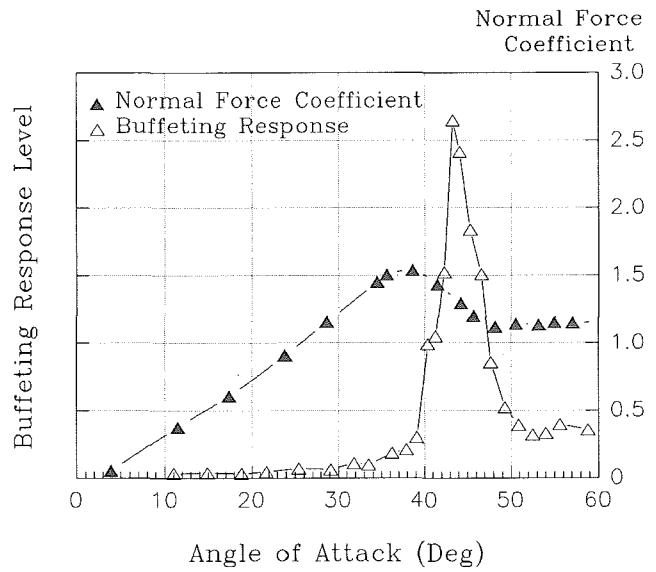


Figure 5: Buffet Profile for Unblown Wing, 1st Bending Mode.

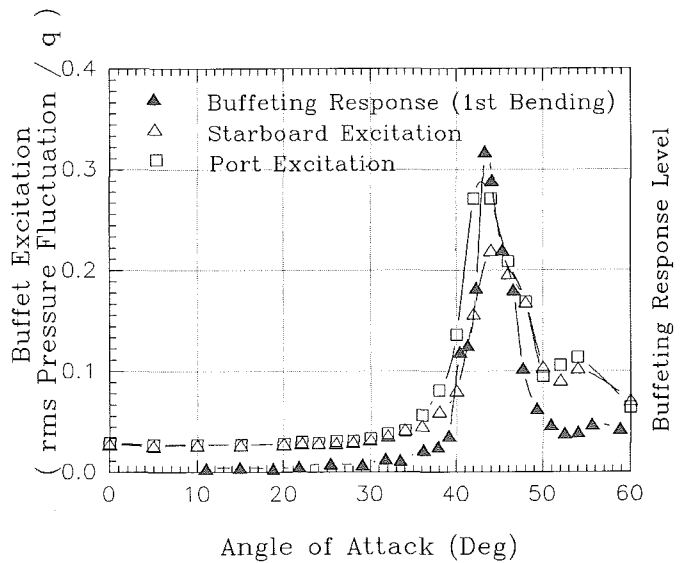


Figure 6: Comparison between Buffet Excitation and Response for Unblown Wing, 1st Bending Mode.

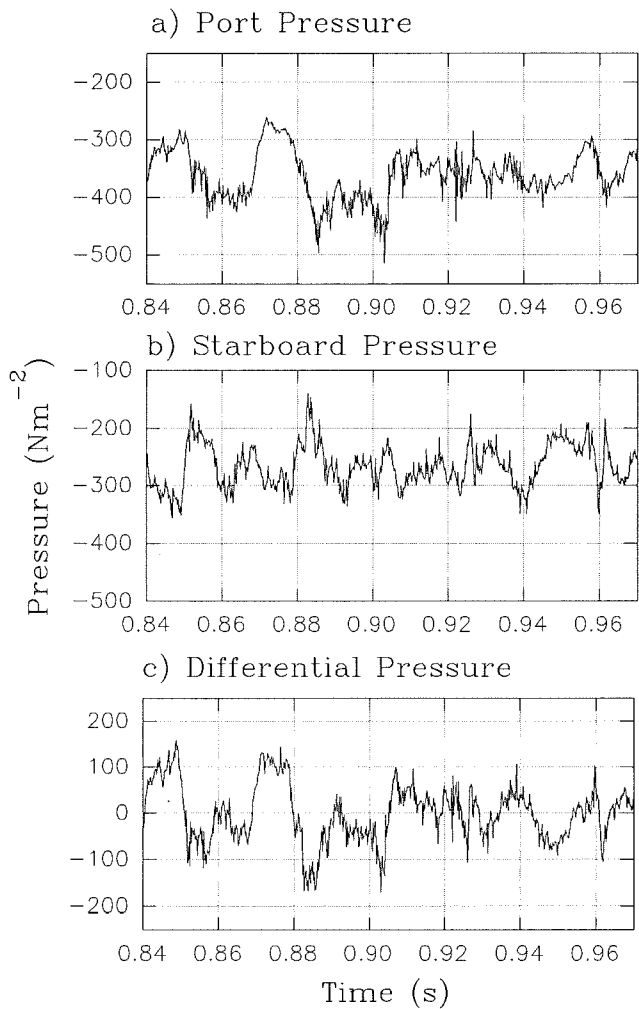


Figure 7: Unsteady Pressure Traces,  $\alpha=44^\circ$ .  
 a) Port Pressure  
 b) Starboard Pressure  
 c) Fin Differential Pressure.

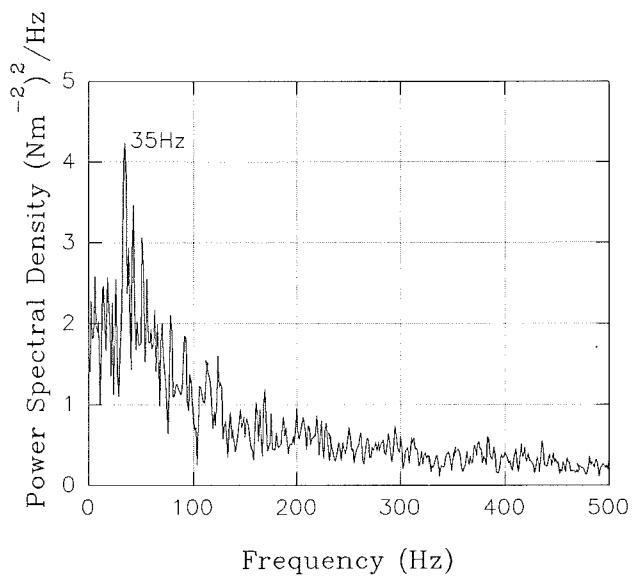


Figure 9: Power Spectral Density of Fin Differential Pressure, Unblown Wing,  $\alpha=44^\circ$ .

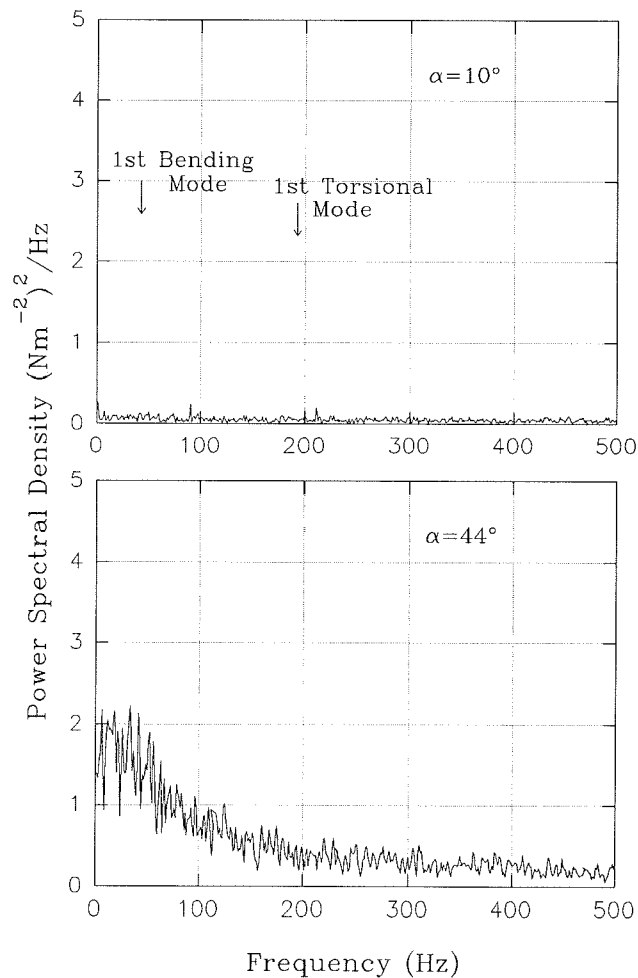


Figure 8: Power Spectral Density, Unblown Wing:  
 a)  $\alpha=10^\circ$   
 b)  $\alpha=44^\circ$ .

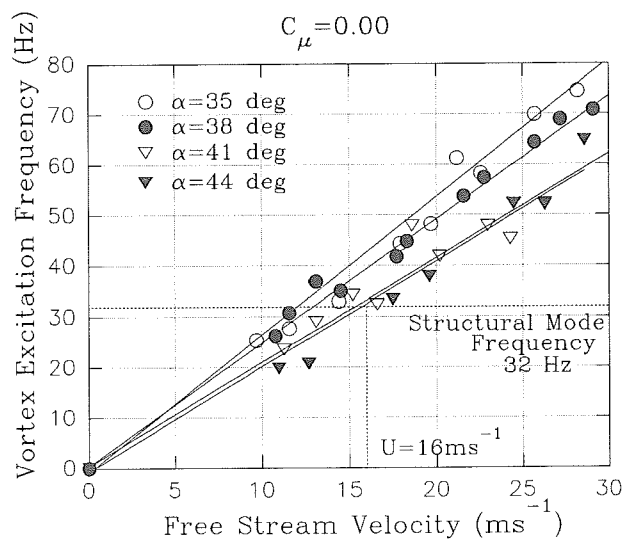


Figure 10: Variation of Vortex Excitation Frequency with Free Stream Velocity, Unblown Wing.



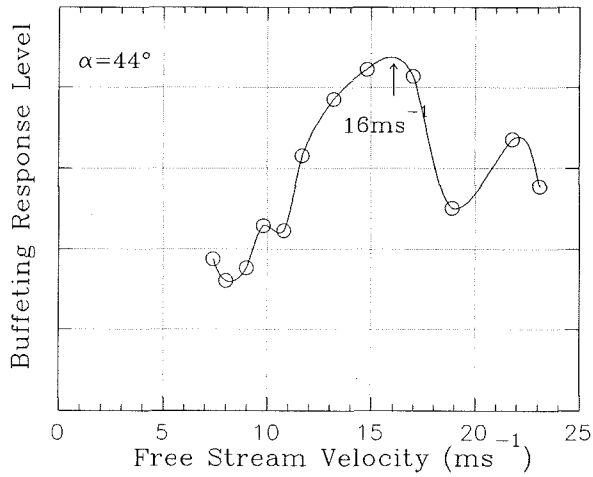


Figure 11: Variation of Buffeting Response with Free Stream Velocity, Unblown Wing.

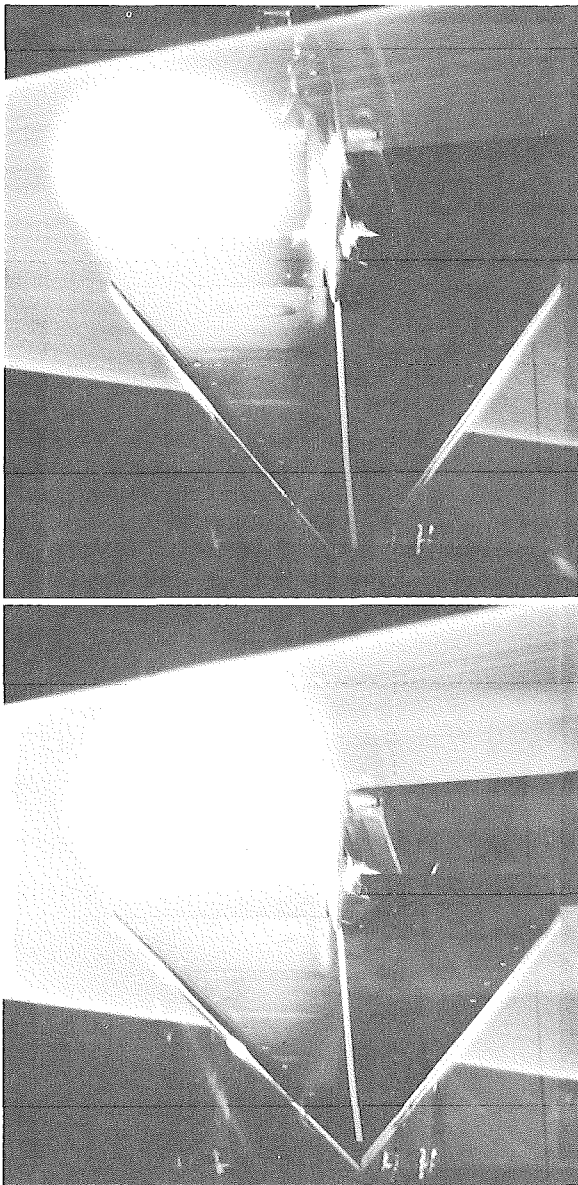


Figure 12: Laser Light Sheet Flow Visualisation, Unblown Wing:  
 a)  $\alpha = 36^\circ$   
 b)  $\alpha = 43^\circ$ .

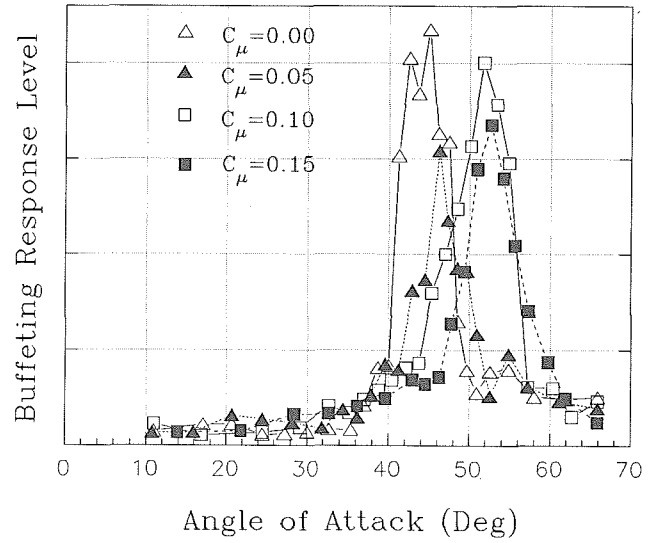


Figure 13: Effect of Blowing Momentum Coefficient on Buffet Profiles for Blown Wing, 1st Bending Mode, Parallel Slot Distribution.

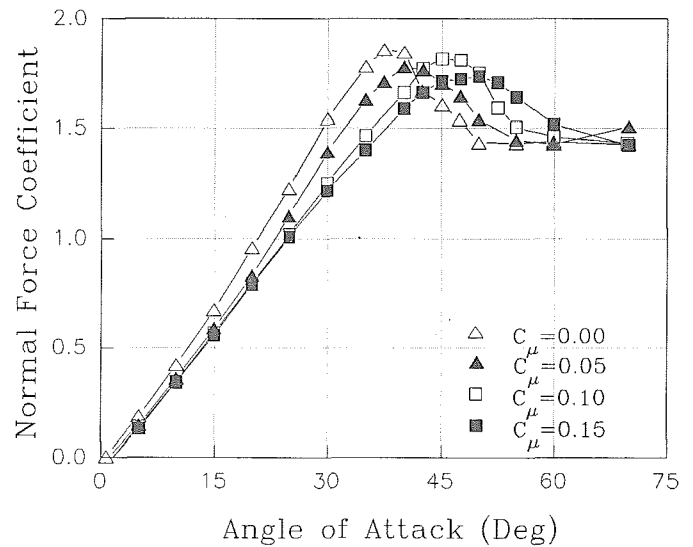


Figure 14: Effect of Blowing Momentum Coefficient on Normal Force, Blown Wing.

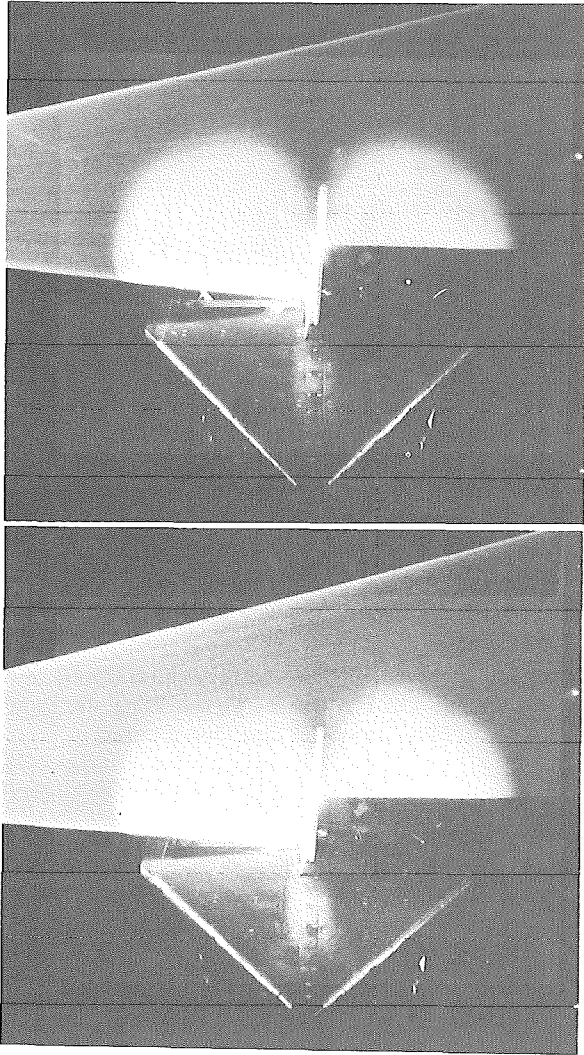


Figure 15: Laser Light Sheet Flow Visualisation, Blown Wing:  
 a)  $\alpha=44^\circ$ ,  $C_\mu=0.00$   
 b)  $\alpha=47^\circ$ ,  $C_\mu=0.05$

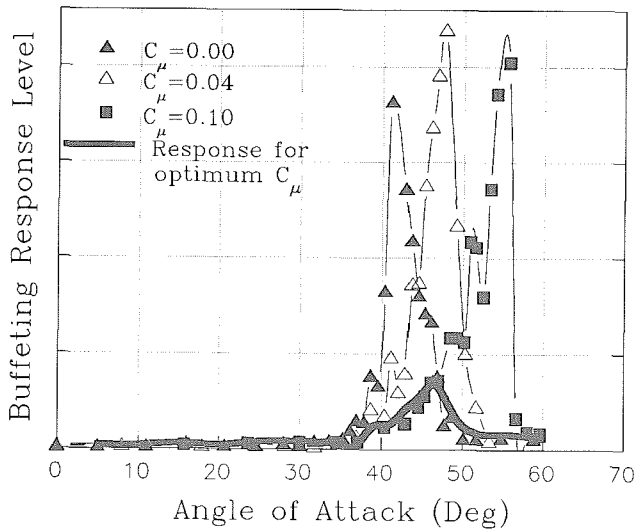


Figure 16: Effect of Blowing Momentum Coefficient on Buffet Profiles for Blown Wing, 1st Bending Mode, Tapering Slot Distribution.

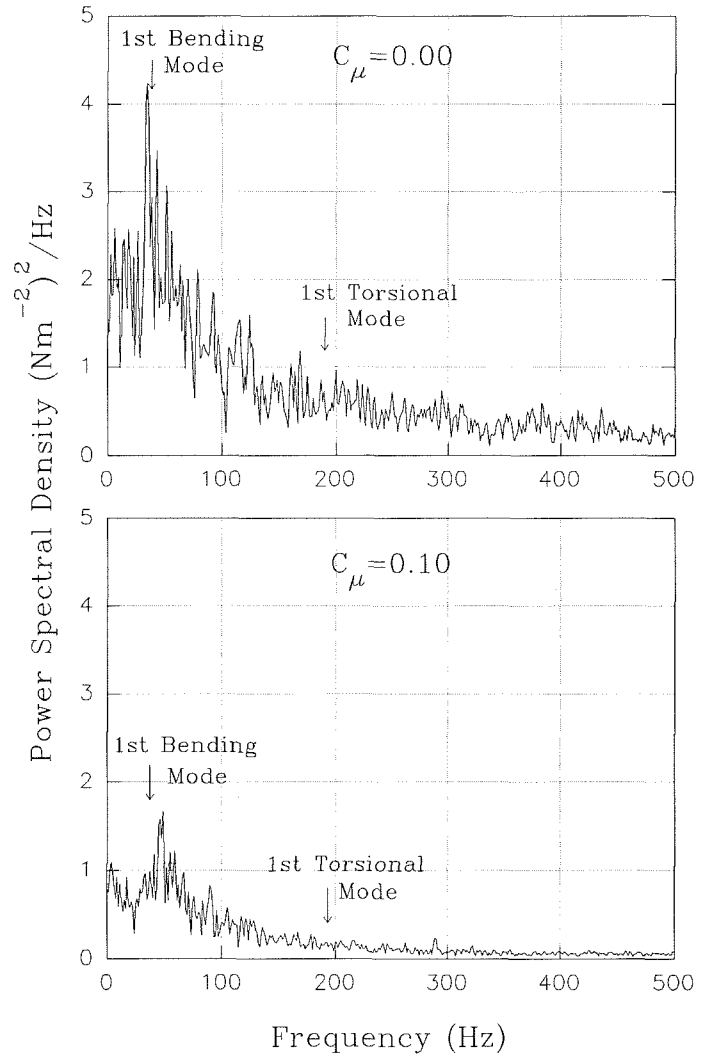


Figure 17: Effect of TLEB on Power Spectral Densities,  $\alpha=44^\circ$ .  
 a)  $C_\mu=0.00$   
 b)  $C_\mu=0.10$

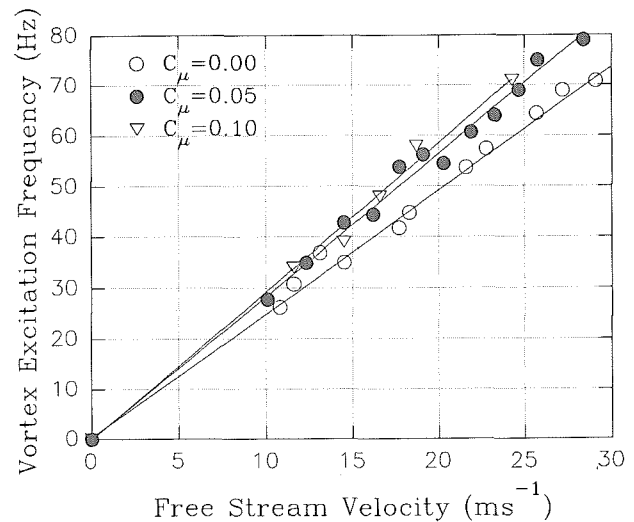


Figure 18: Effect of Symmetric TLEB on Vortex Excitation Frequencies.